

Absorption spectrum of clusters of spheres from the general solution of Maxwell's equations. The long-wavelength limit

J. M. Gérardy and M. Ausloos

Institut de Physique, B5, Université de Liège, B-4000 Sart Tilman/Liège 1, Belgium

(Received 17 December 1979)

A theory is presented to calculate the infrared absorption spectrum of N dielectric spheres of arbitrary sizes, embedded in a dielectric matrix. The Laplace equation is solved exactly for this system, and general solutions take into account interactions at all multipolar orders. Phase factors are introduced when retardation effects become important. Absorption and absorbed power spectra are calculated for two (different or identical) spheres and for an infinite linear chain of identical spheres for different field directions. The theory is applied to MgO spheres. It is found that the Fröhlich mode for a single sphere splits into several resonant modes, and that quadrupolar-order interactions and incident field direction have drastic effects on the predicted infrared spectrum. Experimental consequences regarding damping-factor effects and the position of the modes are discussed.

I. INTRODUCTION

A large variety of particle sizes, compositions, and environments are met in nature. Among experimental techniques chosen for particle-size measurement and distribution, light scattering allows particle monitoring in the 0.08 to 100 μm range. This encompasses an important part of all "industrial particles." Much work has already been presented on the light scattered by powders, with emphasis on metallic powders.¹ Investigative techniques have made less use of infrared and Raman absorption spectrum analysis, although several approximate theories have been recently presented in particular about infrared absorption in dielectric powders²⁻¹³ (as well as in metals¹). We will report elsewhere on the general solution of Maxwell's equation for a powder, and consider here the particular "long-wavelength limit." We follow the usually acceptable statistical assumption, viz., of spherically symmetric particles.¹⁴⁻¹⁶

Without loss of generality, let us consider the case of an ionic powder in an as yet unspecified matrix. The infrared absorption amplitude $A(\omega)$ (which is proportional to the absorption coefficient in the case of a dilute layer of particles) is expressed in a continuum theory¹² in terms of the imaginary part of the directionally averaged particle susceptibility, $\langle\chi(\omega)\rangle$, by

$$A(\omega) = (2Mv/\pi Nq^2)(\omega/\omega_T) \text{Im}\langle\chi(\omega)\rangle, \quad (1)$$

where M is the reduced mass, v the particle volume ($=4\pi R^3/3$), q the ionic charge, N the number of ion pairs in the microcrystal, ω_T the transverse-optical phonon frequency of the (bulk) material, and

$$\langle\chi(\omega)\rangle = \frac{1}{3} \frac{Nq^2}{Mv} \sum_{\beta,m} \frac{C_{\beta,m}}{\omega_m^2 - \omega(\omega + i\gamma)}, \quad (2)$$

where $C_{\beta,m}$ is the dipolar strength,^{2,12} ω_m the polarization mode frequency, and γ an appropriate (small) damping factor. Although these formulas are typical of "rigid-ion diatomic lattice" theory,^{8,17} substitution of (2) into (1) indicates that the relevant unknown quantities are the ω_m 's. Clearly, most theories have attempted to obtain such values by "brutal" lattice-dynamical calculations. It is of interest to ask whether such values, and hence the absorption spectrum, can be obtained in a continuum approximation, given measured macroscopic quantities characterizing the powder and its matrix, i.e., the respective frequency-dependent dielectric constant $\epsilon_i(\omega)$ and $\epsilon_e(\omega)$. In particular, one can examine the effect of particle interaction in a continuum theory as a function of interparticle distance and radius. In so doing one can check how the single dipolar-active infrared mode for an isolated sphere, the Fröhlich mode,¹⁸ which obeys

$$\epsilon_i(\omega_s) + 2\epsilon_e(\omega_s) = 0, \quad (3)$$

is modified.

We obtain here general formulas giving *all* infrared-active, or not, modes (in principle for any $2l$ polar order) for an arbitrary distribution of spherical particles in the long-wavelength limit, while also taking into account retardation effects. The N -sphere case without retardation is treated in Sec. II. Retardation effects are included in Sec. III. One could perform calculations for arbitrary $2l$ polar order, but for comparison with other work, illustrations of the results are given only for a linear chain of identical spheres and for two spheres of different sizes (Sec. IV). Quadrupolar effects are included in the former case.

In Sec. IV, we present the absorption spectrum for different cases (spheres of equal or unequal

radii, two spheres and the linear chain, with or without damping factor and with or without inclusion of quadrupolar effects). In Sec. V, a brief comparison is made with other work, and some emphasis is placed on new results presented here.

II. INTERACTION BETWEEN SPHERICAL IONIC PARTICLES

A. Single-sphere case

Consider an isolated sphere of radius R and characteristic dielectric constant ϵ_i in a uniform isotropic matrix of dielectric constant ϵ_e . The electric field \vec{E}_i in the sphere can be written in terms of the potential ϕ_i as

$$\vec{E}_i = -\vec{\nabla}\phi_i, \quad (4)$$

$$\phi_i = -E_0 \sum_{n,m} a_{nm} H_{nm}(r, \theta, \varphi), \quad (5)$$

with

$$H_{nm}(r, \theta, \varphi) = r^n Y_{nm}(\theta, \varphi), \quad (6)$$

where the $Y_{nm}(\theta, \varphi)$ are the usual spherical harmonics. The potential ϕ_e outside the sphere is

$$\phi_e = -E_0 \sum_{n,m} b_{nm} X_{nm}(r, \theta, \varphi), \quad (7)$$

with

$$X_{nm}(r, \theta, \varphi) = r^{-n-1} Y_{nm}(\theta, \varphi). \quad (8)$$

Also, let the incident radiation field be defined by an electric field

$$\vec{E}_0 = -\vec{\nabla}\phi_0 \quad (9)$$

and a corresponding electrical potential

$$\phi_0 = -E_0 \sum_{n,m} d_{nm} H_{nm}(r, \theta, \varphi). \quad (10)$$

B. N -sphere case

Owing to the presence of neighboring spheres, the field inside and outside a sphere (for example, B) is modified, and its interior potential is hereby called $\phi_i(B)$ with coefficients $a_{nm}(B)$. The potential outside B due to the "incident" potential ϕ_0 and that due to the other (for example, S) spheres is given by

$$\phi_i(B) = \phi_e(B) + \sum_{S \neq B} \phi_e(S) + \phi_0. \quad (11)$$

The usual boundary conditions on the sphere of radius R_B and dielectric constant ϵ_i^B are

$$\phi_i(B)|_{R_B} = \phi_e(B)|_{R_B}, \quad (12)$$

$$\epsilon_i^B \vec{\nabla}\phi_i(B) \cdot \vec{n}|_{R_B} = \epsilon_e \vec{\nabla}\phi_e(B) \cdot \vec{n}|_{R_B}, \quad (13)$$

where \vec{n} is the normal at the surface of sphere B .

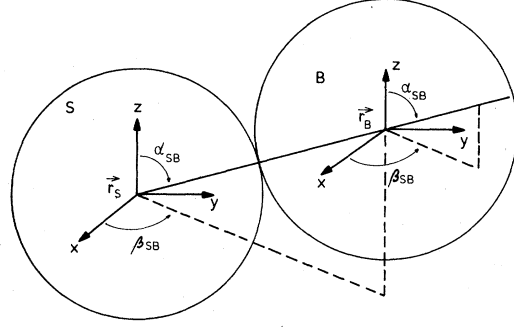


FIG. 1. Reference frame S and B with position vectors \vec{r}_S and \vec{r}_B centered, respectively, on sphere S and B . The center-to-center vector $\vec{r}_B - \vec{r}_S$ is characterized by the angle α_{SB} and the angle β_{SB} with respect to the original fixed reference frame.

The functions $X_{qp}(S)$ described in a frame centered on sphere S can be expressed in terms of functions $H_{nm}(B)$ centered on sphere B as

$$X_{qp}(S) = \sum_{n,m} \langle X_{qp}(S) | H_{nm}(B) \rangle H_{nm}(B). \quad (14)$$

Rewriting the boundary conditions in terms of the above expressions (5), (7), and (10), using (14), and eliminating $a_{nm}(B)$ between these equations leads to a matrix equation for the $b_{nm}(B)$

$$\frac{\epsilon_i^B + [(n+1)/n]\epsilon_e}{(\epsilon_i^B - \epsilon_e)R_B^{2n+1}} b_{nm}(B) + \sum_{S,p,q} b_{qp}(S) \langle X_{qp}(S) | H_{nm}(B) \rangle = -d_{nm}, \quad (15)$$

where the notation $\sum_{S,p,q}$ means $\sum_{S=1}^N \sum_{q=1}^{\infty} \sum_{p=-q}^{+q}$, with $S \neq B$, and

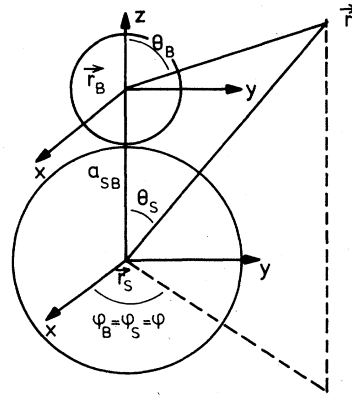


FIG. 2. A point \vec{r} in the space is defined in both rotated frames \vec{r}_S and \vec{r}_B by the polar angles (respectively, θ_S, φ_S and θ_B, φ_B). The common z axis gives here $\varphi_S = \varphi_B$. Notice that spheres S and B are not necessarily touching each other.

$$\langle X_{qp}(S) | H_{nm}(B) \rangle = \frac{\int_{\Omega_B} X_{qp}(\mathbf{r}_S, \theta_S, \varphi_S) H_{nm}^*(\mathbf{r}_B, \theta_B, \varphi_B) d\Omega_B}{\int_{\Omega_B} |H_{nm}(\mathbf{r}_B, \theta_B, \varphi_B)|^2 d\Omega_B}, \quad (16)$$

which is, in fact, the hardest part to calculate.

In order to do so, it is necessary to express the $Y_{qp}(\theta_S, \varphi_S)$ spherical harmonics in the B reference frame. All frames are chosen with each axis parallel to a general reference frame. First, both reference frames S and B are rotated around the z axis by the same angle β_{SB} , then around the

y axis by the same angle α_{SB} , in order to obtain two new frames with a common z axis (see Fig. 1).

The relation between the spherical harmonics of the original system and the final system can be written using Jeffrey's theorem¹⁹

$$Y_{nm}(\theta_S, \varphi_S) = e^{im\beta_{SB}} \sum_{l=-n}^{+n} O(n, m, l, \alpha_{SB}) Y_{nl}(\theta_B, \varphi_B), \quad (17)$$

with

$$O(n, m, l, \alpha) = (-1)^{n+l} [(n+m)!(n-m)!(n+l)!(n-l)!]^{1/2} \sum_{r=f}^g \frac{(-1)^r (\cos \frac{1}{2}\alpha)^{2r+m+l} (\sin \frac{1}{2}\alpha)^{2(l-r)-m-l}}{r!(n-m-r)!(n-l-r)!(m+l+r)!}, \quad (18)$$

where $f = \max(0, -m-l)$ and $g = \min(n-l, n-m)$. Taking into account the distance between reference frames, it is now easy to relate the spherical harmonics in different frames,

$$\frac{Y_{nm}(\theta_S, \varphi_S)}{|\vec{\mathbf{r}}_S - \vec{\mathbf{r}}_B|^{n+1}} = \frac{(2n+1)^{1/2}}{[(n+m)!(n-m)!]^{1/2}} \sum_{k=|m|}^{\infty} (-1)^{k+m} \frac{(n+k)! Y_{km}(\theta_B, \varphi_B)}{[(2k+1)(k-m)!(k+m)!]^{1/2}} \frac{|\vec{\mathbf{r}}_S - \vec{\mathbf{r}}_B|}{a_{SB}^{n+k+1}}. \quad (19)$$

(see Fig. 2 for definition of parameters.)

Using (16), (17), (19), and standard orthogonality relations for the spherical harmonics,

$$\int_{\Omega} Y_{lm}(\theta, \varphi) Y_{l'm'}^*(\theta, \varphi) \sin\theta d\theta d\varphi = \delta_{lq} \delta_{mp}, \quad (20)$$

where δ_{lq} is the Kronecker delta function, we obtain

$$\langle X_{qp}(S) | H_{nm}(B) \rangle = \frac{(-1)^n (q+n)!}{a_{SB}^{q+n+1}} \left(\frac{2q+1}{2n+1} \right)^{1/2} e^{i(p-m)\beta_{SB}} \sum_{l=-q}^{+q} \frac{(-1)^l O(q, p, l, \alpha_{SB}) O(n, m, l, \alpha_{SB})}{[(n+l)!(n-l)!(q+l)!(q-l)!]^{1/2}}, \quad (21)$$

which, substituted into (15), allows one to describe the field outside the spheres in the absence of retardation effects. Equation (15) consists of a generalization to arbitrary clusters of the method proposed by McKenzie *et al.*²⁰ and by McPhedran *et al.*²¹ for calculating the static properties of lattices of polarizable spheres.

III. RETARDATION EFFECTS

The neglect of retardation effects is valid as long as the spheres are close to each other, i.e., $|k_e a_{SB}| \ll 1$, where k_e is the wave number in the matrix. Nevertheless, situations arise in which the intersphere distance is very large (inter-

stellar medium) or the incident radiation contains small wavelengths and the field oscillates between distant spheres. In such a case, $|k_e a_{SB}|$ is not negligible with respect to unity. The phase of the incident field and of the diffracted field must be taken into account, and phase factors must be introduced in each term of Eq. (15). The new equation, being much more complex, is not written here but will be discussed in a later work.

However, assuming that (1) the phase of the incident field on the sphere is equal to that at the sphere center, and (2) the phase difference between diffracted fields by different spheres is that between the sphere centers, Eq. (15) is easily modified to read

$$\frac{\epsilon_i^B + [(n+1)/n]\epsilon_e}{(\epsilon_i^B - \epsilon_e)R_B^{2n+1}} b_{nm}(B) + \sum_{S,p,q} b_{qp}(S) \langle X_{qp}(S) | H_{nm}(B) \rangle e^{ik_e a_{SB}} = -d_{nm} e^{i\vec{k}_e \cdot \vec{r}_B}. \quad (22)$$

The above assumptions are strictly valid for "point spheres" and, by extension, for slowly varying fields inside and outside each sphere:

$|k_i^B R_B| \ll 1$ and $|k_e R_B| \ll 1$, where k_i^B is the wave number in the B sphere. Typically, we have $R_B \leq 1000 \text{ \AA}$.

IV. EXAMPLES

A. Linear chain, identical spheres, regularly spaced

As shown elsewhere, chains of identical spheres are seen in pictures of powders¹⁶ and are representative of the structure of a real powder.¹⁰ Their study can give a good idea of the bounds and shape of the infrared spectrum.

We suppose the chain to be parallel to the z axis. We consider only the long-wavelength-limit case (i.e., $|\vec{k}_e| = 0$), but we will look for cases corresponding to a different polarization mode of the incident field. We can write, using (21),

$$\sum_{S \neq B} \langle X_{qp}(S) | H_{nm}(B) \rangle = \frac{(q+n)! [(-1)^q + (-1)^n] \delta_{m,p}}{[(n+p)!(n-p)!(q+p)!(q-p)!]^{1/2}} \times \frac{(2q+1)^{1/2} (-1)^p \zeta(q+n+1)}{(2n+1)^{1/2} a^{q+n+1}}, \quad (23)$$

where a is the distance between the centers of two neighboring spheres and $\zeta(n)$ is the Riemann zeta function.²²

By symmetry, all the spheres oscillate in phase: $b_{nm}(S) = b_{nm}(B) = b_{nm}$ in such a limit. In order to solve Eq. (15), the sum in the left-hand side (i.e., the development of the diffracted field) is limited to a given polar order (here to the quadrupolar order, $n \leq 2$). The matrix equation is separable into two parts, one involving the dipolar modes only, the other the quadrupolar modes only. The resulting resonant frequencies are a superposition of two independent equations.

The dipolar modes ω_{1m} are found from the poles of the expression giving b_{1m} , i.e., from

$$\epsilon_i(\omega_{1m}) = -2\epsilon_e(\omega_{1m}) \frac{(a/R)^3 + j_{1m}\zeta(3)}{(a/R)^3 - 2j_{1m}\zeta(3)}, \quad (24a)$$

where $\zeta(3) = 1.2021$ and j_{1m} takes the values -1 for $m = \pm 1$, and $+2$ for $m = 0$. Similarly, the frequencies of the quadrupolar modes, ω_{2m} , are obtained from the poles of b_{2m} or from

$$\epsilon_i(\omega_{2m}) = -\frac{3}{2}\epsilon_e(\omega_{2m}) \frac{(a/R)^5 - \frac{2}{3}j_{2m}\zeta(5)}{(a/R)^5 + j_{2m}\zeta(5)}, \quad (24b)$$

where $\zeta(5) = 1.0369$ and j_{2m} takes the values 2 for $m = \pm 2$, -8 for $m = \pm 1$, and $+12$ for $m = 0$.

Fuchs¹² has shown that the use of the bulk-material dielectric constant $\epsilon_i(\omega)$ is a good approximation for describing the true dielectric constant of cubic dielectric particles. For testing our method, we have thus taken a well-known model dielectric constant

$$\epsilon_i(\omega) = \epsilon_\infty + (\epsilon_0 - \epsilon_\infty) \frac{\omega_T^2}{(\omega_T^2 - \omega^2)}, \quad (25)$$

extending Fuchs results to spherical shapes.

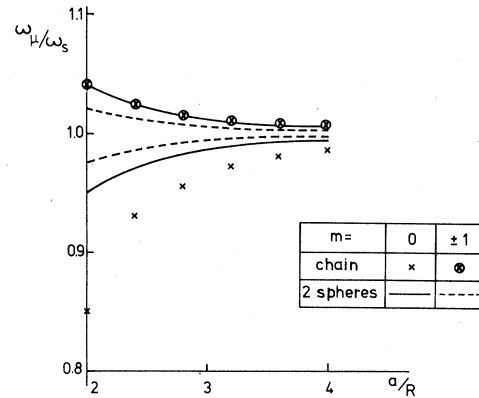


FIG. 3. Ratio of the dipolar resonant frequency ω_μ and the usual noninteracting single-particle Fröhlich frequency ω_s as a function of the interparticle distance measured in sphere radius R units for MgO particles. Crosses and \otimes correspond to equal-size spheres linear-chain resonant modes. Solid and dashed lines correspond to the two-sphere cluster ($R^2 = R_1 R_2$). The inner mode (dashed line) are doubly degenerate.

In Fig. 3, the crosses and \otimes show the variation of the dipolar mode frequencies $\omega_\mu (= \omega_{1m})$ as a function of the ratio a/R for the case of a linear chain of MgO spheres in vacuum; ω_s is the Fröhlich frequency and $\omega_L (= \omega_T)$ is the longitudinal (transverse) plasmon bulk resonance given by $\epsilon_i(\omega_L) = 0$ [$\epsilon_i(\omega_T) = \infty$]. For MgO we have taken $\epsilon_0 = 9.8$, $\epsilon_\infty = 2.95$, $\omega_T = 7.5 \times 10^{13} \text{ s}^{-1}$, $\omega_L = 13.67 \times 10^{13} \text{ s}^{-1}$, and $\omega_s = 11.58 \times 10^{13} \text{ s}^{-1}$.

When the incident uniform field is parallel to the axis of the chain, the $m = 0$ mode (longitudinal polarization of the field) is the only active one. When the field is normal to the chain axis (transversal polarization) only the degenerate mode $m = \pm 1$ is active. In Fig. 4, we have given the variation of the quadrupolar mode frequencies $\omega_\mu (= \omega_{2m})$ as a function of the ratio a/R in the same cases as in Fig. 3. The mode multiplicity is indicated. All these modes are nonactive in a uniform incident field. The characteristic frequency ω_Q of the so-called quadrupolar mode of a single sphere is defined by

$$\epsilon_i(\omega_Q) = -\frac{3}{2}\epsilon_e(\omega_Q) \quad (26)$$

[viz., taking the limit $a \rightarrow \infty$ in Eq. (24b)] and serves as a normalizing frequency.

B. Two spheres with different radius

Limiting Eq. (15) to the dipolar order ($n \leq 1$) and neglecting retardation effects again, we obtain the resonant modes by solving

$$\prod_{s=1}^2 [\epsilon_i^{(s)}(\omega) + 2\epsilon_e^{(s)}(\omega)] = \frac{R_1^3 R_2^3}{a^6} j_m \prod_{s=1}^2 [\epsilon_i^{(s)}(\omega) - \epsilon_e(\omega)], \quad (27)$$

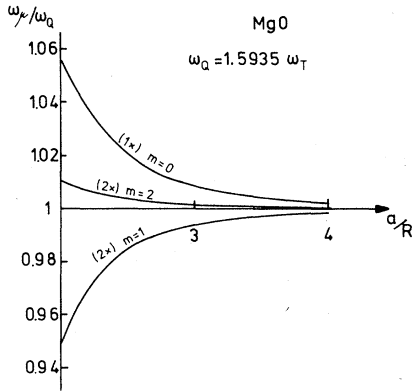


FIG. 4. Quadrupolar resonance frequency ω_μ vs a/R ratio in the case of a linear chain of equal-size MgO spheres (radius R , distance a). The mode multiplicity is given in parentheses; the number m characterizes the azimuthal part of the spherical harmonics.

where $\epsilon_i^{(s)}(\omega)$ is the dielectric constant of the s th sphere and $j_m = -1$ for $m = \pm 1$, and $j_m = 2$ for $m = 0$.

The solutions of (27) have been calculated in the case of two MgO spheres and are shown in Fig. 3. Notice that the downward shifts of the Fröhlich mode are much smaller than those of the linear chain, but the upward shifts have similar magnitudes. As in the case of the chain, the modes $m = 0$ are active only for a longitudinal polarization of the field, while the modes $m = \pm 1$ are active for a transverse polarization. Notice that when $R_1 = R_2$, the upper frequency mode in the longitudinal polarization geometry and the lower frequency mode in the transverse polarization case are always nonactive. Only one mode is thus active in such a case ($R_1 = R_2$) for a given polarization. The quadrupolar modes are more complicated to obtain and are left for further work.

V. OPTICAL ABSORPTION

In order to describe the absorption spectrum of a powder we can consider either the absorption coefficient, as defined in (1), or the total absorbed power. For the former quantity, we calculate an "averaged susceptibility" using the average polarization of each sphere. This form takes into account the interaction of neighboring spheres through the results of Sec. III.

The polarization density can be written as

$$\vec{p}(\vec{r}_B, \omega) = [(1 - \epsilon_i^B)/4\pi] \vec{E}_i(\vec{r}_B, \omega), \quad (28)$$

where \vec{r}_B is the radial vector described in the frame centered on the B sphere. We define the average electrical moment for the B particle as

$$\vec{P}_B(\omega) = \int_{v_B} \vec{p}(\vec{r}_B, \omega) d\vec{r}_B, \quad (29)$$

where the integration is taken over the volume v_B of the sphere. Average normal and parallel susceptibilities are defined by

$$\vec{P}_B(\omega) = v_B [\chi_{\parallel}(B, \omega) \vec{1}_{\parallel} + \chi_{\perp}(B, \omega) \vec{1}_{\perp}] E_0, \quad (30)$$

where $\vec{1}_{\parallel}$ and $\vec{1}_{\perp}$ are unit vectors, respectively, parallel and perpendicular to the incident field \vec{E}_0 . Only $\chi_{\parallel}(B, \omega)$ is discussed here. From (28), (29), and (30), we have

$$\chi_{\parallel}(B, \omega) = \frac{1}{v_B} \frac{1 - \epsilon_i^B}{4\pi E_0} \int_{v_B} \vec{E}_i(\vec{r}_B, \omega) \cdot \vec{1}_{\parallel} d\vec{r}_B. \quad (31)$$

Notice that when $\vec{E}_i(\vec{r}_B, \omega)$ is uniform over the volume v_B , (31) corresponds to the Fuchs's macroscopic definition of the susceptibility.

From the calculation made in Sec. II, one can easily obtain

$$a_{nm}(B) = -[(2n+1)/n] [\epsilon_e / (\epsilon_i^B - \epsilon_e)] \times R_B^{-2n-1} b_{nm}(B). \quad (32)$$

Applying Gauss theorem, using expression (5) for the potential inside the sphere, and orthogonality relations (20) for the spherical harmonics, we obtain from (31) and (32)

$$\chi_{\parallel}(B, \omega) = \left(\frac{3}{4\pi}\right)^{3/2} \epsilon_e [\epsilon_i^B(\omega) - 1] / [\epsilon_i^B(\omega) - \epsilon_e] R_B^{-3} \times \{2^{-1/2} \sin\alpha [b_{11}(B)e^{i\beta} - b_{1-1}(B)e^{-i\beta}] + (\cos\alpha) b_{10}(B)\}, \quad (33)$$

where α and β are spherical angles defining the direction of the incident field in the Cartesian frame centered on sphere B (see, e.g., Fig. 1). Because

$$\chi_B(0) = (1/4\pi) [(\omega_{LB}/\omega_{TB})^2 - 1], \quad (34)$$

where ω_{LB} (ω_{TB}) is the longitudinal (transverse) phonon frequency, we can rewrite (1) as

$$A_{\parallel}(B, \omega) = 8\omega\omega_{TB}/(\omega_{LB}^2 - \omega_{TB}^2) \text{Im}\chi_{\parallel}(B, \omega). \quad (35)$$

The absorption can be deduced immediately from (33) and (35). For N (different or not) spheres, the total absorption is

$$A_{\parallel}(\omega) = \sum_{B=1}^N \xi_B A_{\parallel}(B, \omega), \quad (36)$$

where ξ_B is a normalization factor taking into account the particle volume (hence the polarization moment density),

$$\xi_B = v_B/v, \quad (37)$$

$$v = \sum_{S=1}^N v_S. \quad (38)$$

We show in Fig. 5 the absorption $A_{\parallel}(\omega)$ for the case of two unequal-size MgO spheres for different field incidences and arbitrary damping fac-

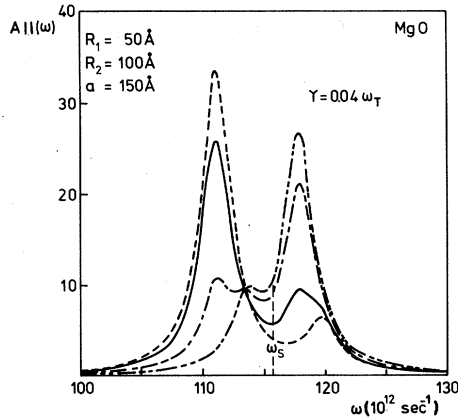


FIG. 5. Absorption $A_{||}(\omega)$ for two touching different MgO spheres ($R_2=2R_1=100 \text{ \AA}$) as a function of frequency. The damping factor γ is chosen equal to $0.04 \omega_T$. Curve --- is given for a field direction such that the angle α between the center-to-center axis and the incident field \vec{E}_0 is $\alpha=0$; curve —: $\alpha=\pi/6$; curve - · - · -: $\alpha=\pi/3$; and curve - · - · -: $\alpha=\pi/2$. ω_S is the Fröhlich resonant mode.

tor ($\gamma=0.04\omega_T$), with the b_{ij} 's calculated taking into account the dipolar terms only. In Fig. 6, we show the absorption $A_{||}(\omega)$ for two equal-size MgO spheres, but with the b_{ij} 's calculated taking into account the quadrupolar ($n=2$) terms.

On the other hand, the total power W absorbed

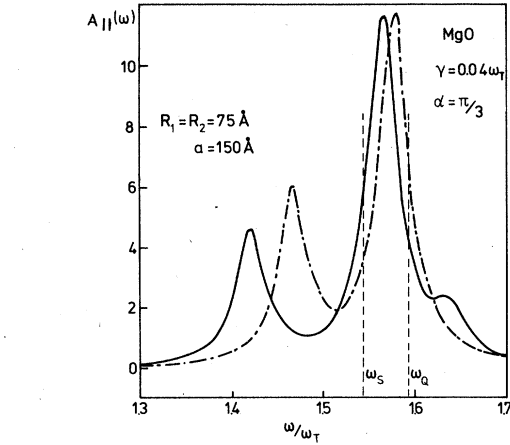


FIG. 6. Absorption $A_{||}(\omega)$ for two touching equal-size MgO spheres (radii $R_1=R_2=75 \text{ \AA}$). The damping factor γ is $0.04 \omega_T$. The incidence angle α of the field \vec{E}_0 is $\pi/3$. Curve - · - · is obtained by limiting equations up to dipolar terms, and curve — takes into account dipolar and quadrupolar interaction as well.

by the spheres can be obtained from the electric field distribution in the particles, i.e., for particle B , we have

$$W(B, \omega) = \epsilon_i^B(\omega) \int_{v_B} |\vec{E}_i(B, \omega)|^2 d\vec{r}_B / (\epsilon_e E_0^2) \quad (39)$$

in reduced units, which for N spheres sums up to

$$W(\omega) = \frac{1}{v} \sum_{B=1}^N W(B, \omega) = \frac{3}{(4\pi v)} \sum_{B=1}^N \frac{\epsilon_e \epsilon_i^B(\omega)}{|\epsilon_e - \epsilon_i^B(\omega)|^2} \left(\sum_{n=1}^{\infty} \frac{(2n+1)^2}{n} R_B^{-2n-1} \sum_{m=-n}^n |b_{nm}(B)|^2 \right). \quad (40)$$

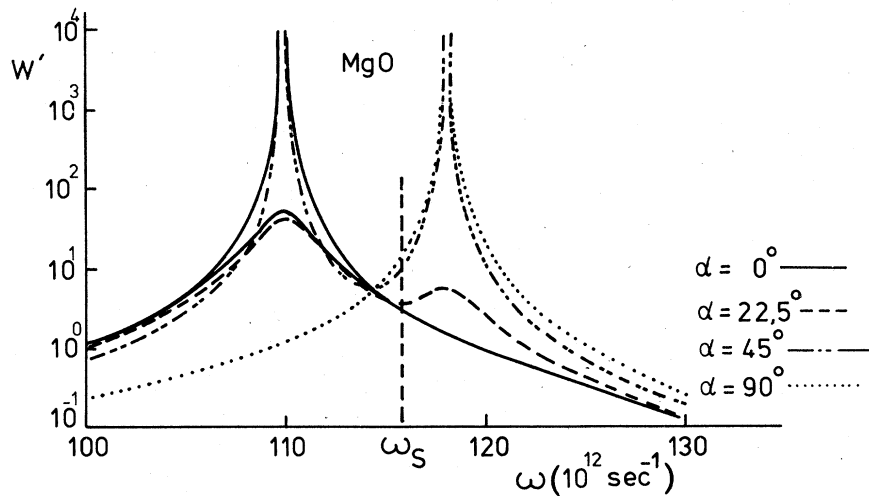


FIG. 7. Reactive power W' as a function of frequency ω for two values of the damping factor ($\gamma=0$: infinite-peak curves; $\gamma=0.04 \omega_T$: finite-maximum curves) for two touching MgO spheres with equal radius $R=75 \text{ \AA}$. Different angles α are considered and indicated on the figure.

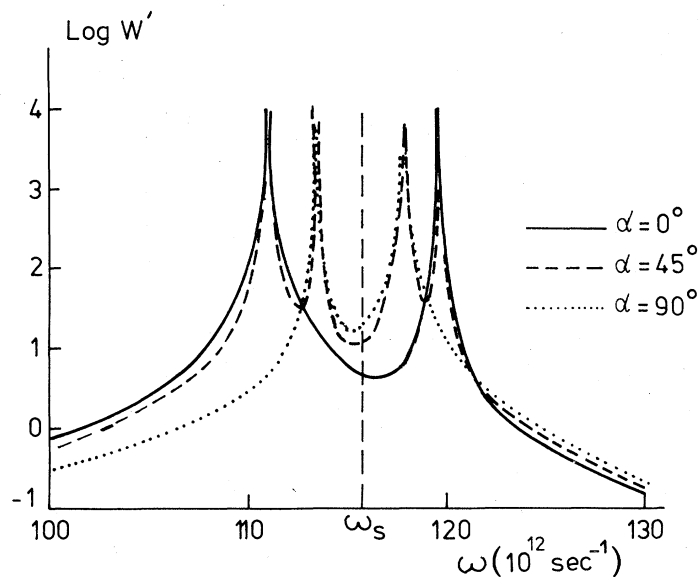


FIG. 8. Reactive power $W'(\omega)$ for two unequal-size MgO spheres ($R_2 = 2R_1 = 75 \text{ \AA}$, $a = 150 \text{ \AA}$) with $\gamma = 0$. The incident field directions α are indicated.

The active and reactive power are, respectively, defined by $\text{Im}W = W''$ and $\text{Re}W = W'$. In absence of damping, the active power W'' vanishes, while the absorption spectrum consists of delta functions. The reactive power W' as seen from Eq. (40) is a linear function of the real part of the dielectric constant $\epsilon'(\omega)$ times a complicated function of the frequency. It can be as usual related to the imaginary part of the dielec-

tric constant, through Kramers-Kronig relations, and hence to experimental data.

The reactive power W' has been calculated in the dipolar approximation ($n \leq 1$) for two MgO spheres of equal sizes for four different field incidences and different damping factors ($\gamma = 0$, or $\gamma = 0.04\omega_T$) (Fig. 7). On Figs. 8 and 9, the reactive power of two *unequal-size* MgO spheres is shown as a function of ω , for different damping

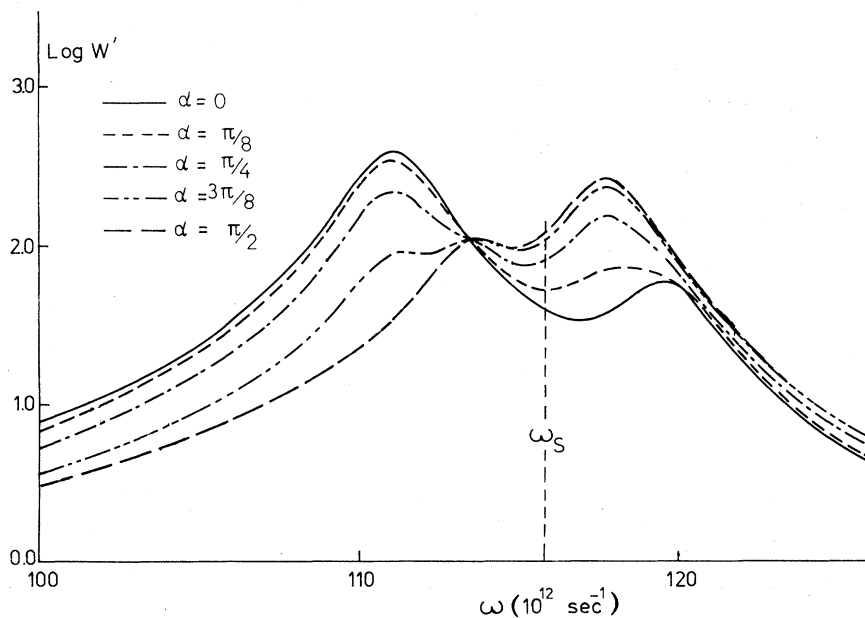


FIG. 9. Reactive power $W'(\omega)$ in the same case as that of Fig. 6 for different angles α . Equations are limited up to dipolar terms. The damping factor γ is chosen to be equal to $0.04\omega_T$.

factors, and for different field incidences.

VI. DISCUSSION

The most important improvement of our work over previous theories is the inclusion of the effect of all $2l$ polar modes on the dipolar resonant modes and on the dipolar absorption spectrum. Furthermore, the method is general enough to permit the calculation of absorption modes and the absorption spectrum of any distribution of spheres in a medium as long as their dielectric constant and radius are known. The full calculation needs much computer work and has not yet been attempted. In fact, it is necessary to know powder statistics before analyzing a given spectrum. The inverse problem (obtaining the statistics from the spectrum) seems, after this stage, partially feasible when the spherical shape approximation is removed.

We will discuss successively:

(a) the effect of the incident field direction on the absorption,

(b) the position of dipolar modes with and without quadrupolar effects,

(c) the possible generalization of implicit formulas giving the mode positions when higher multipolar orders are included,

(d) the damping-factor influence on the spectrum,

(e) the influence of the shape or size of the particles.

For a cluster of two identical spheres, both absorbing modes were already found by Clippe *et al.*⁴ However, the position of the four resonant modes predicted by (27), when the spheres have unequal size, is a new result. Notice the drastic effect of the incident field direction (with respect to the center-to-center axis) on the absorption amplitude and absorbed power spectrum.

Longitudinal absorption modes only appear when the "excitation" is parallel to the common axis of both spheres, while transverse modes appear when \vec{E} is perpendicular to this axis. As this observation also holds true for the spectral bounds of the linear chain, one can easily imagine how useful the observation of a powderlike system would be in polarized light. This would lead to some knowledge of the configurations of spheres in clusters.

However, before one can be fully certain about this point, it is necessary to have a precise idea of the position of the resonant dipolar modes. Our work in Secs. III and IV indeed indicates that an appreciable shift in the *theoretical* mode position occurs according to the level of accuracy imposed on the solution of Maxwell's equations.

We have indeed indicated in Fig. 6 the important displacement of the mode when quadrupolar terms are taken into account in calculating the b_{nm} 's and the ω_m 's. It would be of interest to examine whether the "motion" of the modes toward lower and upper values is asymptotic or not. The answer is beyond the scope of this paper and is left for future work.

Furthermore, the appearance of low shoulders in the upper part of the spectrum is a new feature which requires extension of this work. The variation of dipolar modes as a function of a/R has already been examined, e.g., by Ronveaux *et al.*²³ Their results agree with ours, although some approximation (at the final stage) leads them into completely missing the $m=0$ mode. These authors indeed take into account only the multipolar fields for which $n=|m|$, with $n \geq 1$. The power-law variation of ω vs a/R is identical to ours, however. In the Appendix, we correct the *a priori* truncation of the field equations by Ronveaux *et al.*²³ and recover our results.

An interesting point concerns the implicit equations allowing the extraction of the dipolar and quadrupolar ($|\vec{k}_e|=0$) resonant modes [i.e., Eqs. (24) and (25), and their generalization to higher-order modes of the linear chain]. Preliminary results indicate that the form of the equations is more complicated and cannot be written *in general* as

$$\epsilon_i(\omega_{lm}) = -\frac{l+1}{l} \epsilon_e(\omega_{lm}) \frac{(a/R)^{2l+1} - \alpha_{lj} j_{lm} \zeta(2l+1)}{(a/R)^{2l+1} + \beta_{lj} j_{lm} \zeta(2l+1)}. \quad (41)$$

Inclusion of the octupolar term in the field equations already breaks the "symmetry" of the equations. For the two-sphere cluster, inclusion of quadrupolar terms also leads to a more elaborate form of an implicit equation like (27). Eq. (41) is only exact in the limit of large sphere separation. Nevertheless, it would be interesting to observe on experimental data whether Eq. (41) corresponds to and may serve as some realistic approximation to characteristic mode frequencies.

Another interesting result concerns the influence of the damping factor on the spectrum. Of course, the greater the damping, the broader the spectrum. However, it is remarkable that for any incident field direction, and for a given damping γ , the absorption amplitude (or the absorbed power) has the same magnitude at a particular frequency ω_1^* (ω_2^*) close to the Fröhlich frequency (see Figs. 5 and 9). Therefore, a change in incident field direction and observation of ω_1^* (ω_2^*) would allow a determination of the experimental parameter γ . We have obtained, in the dipolar approximation, an analytic expression for γ as a function of ω_2^*

$$\delta = \frac{1}{f^2} \frac{\epsilon_e^2(4+s)(1-f^2)^2 - 2\epsilon_e\epsilon_\infty(1+s)(f_L^2 - f^2)(1-f^2) - \epsilon_\infty^2(2-s)(f_L^2 - f^2)^2}{(2-s)\epsilon_\infty^2 + 2\epsilon_e\epsilon_\infty(1+s) - \epsilon_e^2(4+s)}, \quad (42)$$

where $f = \omega_2^*/\omega_T$, $f_L = \omega_L/\omega_T$, $\delta = \gamma/\omega_T$, and $s = (R/a)^3$ for two identical spheres, or $s = 2\zeta(3)(R/a)^3$ for the linear chain ($s \neq 0$).

The variation of ω_2^* with γ is rather weak, however, and does not seem to be observable. This feature of the spectrum remains when higher-order terms are included in the calculation for a single-strand chain of different or identical particles.

The damping factor γ has been an *a priori* parameter introduced into Eq. (25), for example, in order to smooth the spectrum and make it "more realistic." For $\gamma=0$, a complete solution of the field equations would lead to an infinite number of modes [or at least to $N(l+2)$ modes for an N -sphere cluster when the sum in (15) is limited to the $2l$ polar order]. The largest amplitude of the absorption modes would be that for the dipolar modes, followed by that for the quadrupolar modes, etc. The total set of modes would seem to form a continuum. In such a sense, γ can be considered as reproducing (in the dipolar approximation) the effect of higher-order terms. A self-consistent treatment of an effective medium dielectric constant would in fact introduce a real and an imaginary part of the resonant frequencies; the latter part as γ introduces a broadening of the spectrum.²⁴

In usual experimental situations, the particles dispersed in a medium are not truly spherical but have irregular shapes. This causes further substantial broadening of the absorption peaks and spectrum; Fuchs's and Langbein's work^{2,25} on independent cubes has indeed shown that the inclusion of higher-order multipolar terms leads to an additional structure in the absorption spectrum.

According to their results, the strongest absorption is a measure of the equivalent "Fröhlich mode" of the cube. It remains to be discussed how the broadening due to the irregular shape of the particles and that due to the distribution of (spherical) particles in a cluster are affected and in which proportion. Both effects might play a role in reducing the observed "strongest absorption peak" and lead to an erroneous attribution of the mode. Much more work is obviously needed in such a direction.

Finally, even in the framework of our model with "all spherical particles," we can now cover a larger part of the absorption spectrum of a powder by including higher-order multipolar terms.

ACKNOWLEDGMENT

One of us (J. M. G.) would like to thank the Institut pour la Recherche Scientifique dans l'Industrie et l'Agriculture (IRSIA), Brussels, Belgium, for financial support.

APPENDIX

For a linear strand chain, Eq. (18) becomes

$$\begin{aligned} O(n, m, l, o) &= \delta_{ml}, \\ O(n, m, l, \pi) &= (-1)^{n+m} \delta_{m, -l}. \end{aligned} \quad (A1)$$

Consider identical particles of radius R and center-to-center distance a . Inserting (A1) into expression (21) and limiting Eq. (15) for $|m| \geq 1$ to $n=q=m$, i.e., following the Ronveaux *et al.*²³ approximations, we obtain

$$\frac{n\epsilon_i(\omega) + (n+1)\epsilon_e(\omega)}{n[\epsilon_i(\omega) - \epsilon_e(\omega)]} b_{nm}(j) + (R/a)^{2n+1} \sum_{k \neq j} \frac{b_{nm}(k)}{|j-k|^{2n+1}} = -d_{nm} R^{2n+1}, \quad (A2)$$

where j and k are the sphere indices. Modes $n = |m|$ are twice degenerate ($n = |\pm m|$) and are given by Ronveaux's equation

$$\det(M_{nm} - \lambda_{nm} E) = 0, \quad n = |m| \quad (A3)$$

where M_{nm} is the matrix

$$M_{nm} = \begin{pmatrix} 0 & 1^{-\mu} & 2^{-\mu} & \cdots & (N-1)^{-\mu} \\ 1^{-\mu} & 0 & 1^{-\mu} & \cdots & (N-2)^{-\mu} \\ \vdots & \vdots & \vdots & \ddots & \vdots \\ (N-1)^{-\mu} & (N-2)^{-\mu} & (N-3)^{-\mu} & \cdots & 0 \end{pmatrix}, \quad (A4)$$

and where

$$\lambda_{nm} = - \frac{n\epsilon_i(\omega) + (n+1)\epsilon_e(\omega)}{n[\epsilon_i(\omega) - \epsilon_e(\omega)]} \left(\frac{a}{R}\right)^\mu, \quad (A5)$$

with $\mu = 2n+1$. This sort of truncation neglects the $m=0$ (nondegenerate) modes because $n \geq 1$. With the same approximations [Eq. (15) limited up to dipolar terms], the $m=0$ modes are obtained from (A3) and (A4) by adding the condition $M_{10} = M_{11}$ and

$$\lambda_{10} = \frac{1}{2} \frac{\epsilon_i(\omega) + 2\epsilon_e(\omega)}{\epsilon_i(\omega) - \epsilon_e(\omega)} \left(\frac{a}{R}\right)^3, \quad (A6)$$

which differs from λ_{11} by a factor $-\frac{1}{2}$.

Modes $m=0$ are quite important because they lead to a greater splitting than others (see, e.g.,

Fig. 3). Note that all modes (except $n=1$) given by (A3) are nonactive in a uniform field because the d_{nm} 's differ from 0 only when $n=1$.

¹International Meeting on Small Particles and Inorganic Clusters 1976 [J. Phys. (Paris) Colloq. 38, C-2, S7 (1977) and references therein].

²R. Fuchs, Phys. Rev. B 11, 1732 (1975).

³R. Frech, Phys. Rev. B 13, 2342 (1976).

⁴P. Clippe, R. Evrard, and A. A. Lucas, Phys. Rev. B 14, 1715 (1976).

⁵R. Ruppin, Surf. Sci. 58, 550 (1976).

⁶R. Ruppin, Surf. Sci. 51, 149 (1975).

⁷R. Ruppin, Surf. Sci. 62, 206 (1977).

⁸T. P. Martin, Phys. Rev. B 7, 3906 (1973).

⁹R. Ruppin, Phys. Status Solidi. B 87, 619 (1978).

¹⁰M. Ausloos, P. Clippe, and A. A. Lucas, Phys. Rev. B 18, 7176 (1978).

¹¹J. H. Weaver, R. W. Alexander, L. Teng, R. A. Mann, and R. J. Bell, Phys. Status Solidi. A 20, 321 (1973).

¹²R. Fuchs, Phys. Rev. B 18, 7160 (1978).

¹³T. P. Martin and H. Schaber, Phys. Status Solidi B 81, K41 (1977).

¹⁴C. G. Granqvist and N. Calander, Solid State Commun. 31, 249 (1979).

¹⁵F. F. Y. Wang, C. H. Lin, K. C. Yoo, P. J. Herley,

H. Herman, and Y. H. Kao, Philos. Mag. B39, 277 (1979).

¹⁶A. J. Hunt, T. R. Steyer and D. A. Huffman, Surf. Sci. 36, 454 (1973).

¹⁷A. A. Lucas, J. Chem. Phys. 48, 3156 (1968).

¹⁸H. Fröhlich, *Theory of Dielectrics* (Clarendon, Oxford, 1949).

¹⁹B. Jeffreys, Geophys. J. R. Astron. Soc. 10, 141 (1965).

²⁰D. R. McKenzie, R. C. McPhedran, and G. H. Derrick, Proc. R. Soc. London Ser. A 362, 211 (1978).

²¹R. C. McPhedran and D. R. McKenzie, Proc. R. Soc. London Ser. A 359, 115 (1978).

²²M. Abramowitz and I. A. Stegun, *Handbook of Mathematical Functions* (Dover, New York, 1972).

²³A. Ronveaux, A. Moussiaux, and A. A. Lucas, Can. J. Phys. 55, 16 (1977).

²⁴J. E. Gubernatis, *Electrical Transport and Optical Properties of Inhomogeneous Media*, edited by J. C. Garland and D. B. Tanner (AIP, New York, 1977), p. 84.

²⁵D. Langbein, J. Phys. A 9, 627 (1976).